ELSEVIER

Leaf Area Index Estimation from Visible and Near-Infrared Reflectance Data

*John C. Price** *and Walter C. Bausch*†

A two-stream description of the interaction of radiation with vegetation and soil is tested with experimental data for a corn canopy. The results indicate that the two parameters of the theory (reflectance of a dense canopy and the attenuation coefficient for radiation in the canopy) can be estimated for the Thematic Mapper spectral bands. A collection of soil reflectance data is used to develop relationships between near-infrared reflectance and visible reflectances. Jointly the canopy and soil formulations verify the potential for estimating leaf area index from radiation measurements in the visible and near-infrared.

INTRODUCTION

As a fundamental plant parameter leaf area index [LAI = (leaf area) / (ground surface area)] is an important factor in the description of many plant processes, for example, evapotranspiration, photosynthesis, and yield, in addition to its effect on radiation exchange with the atmosphere through its effect on albedo. Leaf area index is an indicator of the density of vegetation, and is relatively easy to measure. In a recent article, Bausch (1993) described the derivation of crop water use coefficients from visible and near-infrared reflectance data, as well as various radiometric vegetation indices such as the normalized difference vegetation index (NDVI) (Rouse et al., 1974) and the soil adjusted vegetation index (SAVI) (Huete, 1988). Measurements of a corn canopy taken above four soils with varying reflectances were used to test the contribution of soil reflectance to remote measurements. Although the implications of radiance derived vegetation indices for surface fluxes and crop growth are many (Wiegand and Richardson, 1990; Hall et al., 1992), in this article only the problem of estimating LAI from reflectance data is addressed.

In previous work Price (1992, to be called P1), developed a methodology for relating visible and near-infrared reflectances to LAI in the presence of variable soil reflectance, and then applied it to satellite data (Price, 1993, to be called P2). The formulation in P1 is based on the two-stream description of the interaction of radiation with the plant canopy and its underlying soil background. This description may oversimplify the radiation problem, since the predicted reflectances depend on only three parameters besides LAI: the reflectance of the soil r_s, the reflectance of a thick (LAI→∞) vegetation canopy r_∞, and the attenuation coefficient for radiation in the canopy c. Both LAI and c are dimensionless. Since soil reflectances are spatially variable an equation relating reflectances at different wavelengths is required to permit solution for LAI from radiance data. The "soil line," which is the relationship between visible and near-infrared reflectance of the underlying soil, is assumed to the known in P1. In P2 the soil line is inferred from satellite data through consideration of a scattergram of reflectance data. This latter procedure is relatively inefficient and does not apply in some cases.

In this article, the experimental data of Bausch (1993) are inserted into the two-stream solution to obtain values of c and r_∞, thereby illustrating that this formulation describes the observed reflectances. Then relationships among visible and near-infrared soil reflectances are derived. These equations are obtained using an ensemble of measured soil reflectance spectra. Together the radiation formulation and soil reflectance equation permit estimation of LAI by radiation measurements of corn in the presence of a variable soil background. A sensitivity analysis is used to show the degree to which experimental errors and questionable assumptions can influence the derived values of LAI for corn.

*Agricultural Research Service, USDA, Beltsville, Maryland
†Agricultural Research Service, USDA, Fort Collins, Colorado
Address correspondence to John C. Price, Remote Sensing Research Laboratory, Building 7, BARC-West, Beltsville, MD 20705.
Received 15 July 1994; revised 26 November 1994.

REMOTE SENS. ENVIRON. 52:55–65 (1995)

655 Avenue of the Americas, New York, NY 10010

0034-4257 / 95 / $9.50
SSDI 0034-4257(94)00111-Y

The present analysis assumes measurements from slightly above the vegetation, so that the effects of the atmosphere are not considered. A summary of previous work on this problem would be very lengthy, but we refer the reader particularly to Clevers (1988; 1989), where a more heuristic approach resembles that used here. References to the extensive earlier literature in the vegetation / radiation / soil problem may be found in the above-cited articles.

ALTERNATIVE VEGETATION INDICES

Vegetation indices based on radiometric measurements have been developed within the remote sensing discipline, while the agronomic community has characterized canopies by LAI, as previously defined. The two are distinguished in the following subsections.

Radiometric Vegetation Indices

A number of mathematical formulas using visible and near-infrared reflectances, here called radiometric vegetation indices, have been proposed for relating radiometric measurements in the visible and near-infrared wavelength intervals to the amount of vegetation present. Perry and Lautenschlager (1984) discussed 15 such radiometric vegetation indices, and formal relationships among them. Recently attention has focused on a commonly used index, the normalized difference vegetation index (NDVI) of Rouse et al. (1974), and a large number of similar formulas. The basis for NDVI is related to the abrupt increase of vegetation reflectance at the wavelength $\lambda = \lambda_0 \simeq 0.7$ μm. This increase may be expressed by the formula

$$\text{NDVI} = \Delta \ln[R(\lambda_0)] = \frac{R(\lambda_0 + \delta\lambda) - R(\lambda_0 - \delta\lambda)}{R(\lambda_0 + \delta\lambda) + R(\lambda_0 - \delta\lambda)} \equiv \frac{R_2 - R_1}{R_2 + R_1}, \quad (1)$$

where $\delta\lambda$ is of the order of 0.1–0.2 μm, and the visible and near-infrared reflectances [$R_1 = R(\lambda_0 - \delta\lambda)$, $R_2 = R(\lambda_0 + \delta\lambda)$] may be obtained by remote measurements from a number of satellites, such as Landsat, SPOT, and the NOAA series, after division by the solar constant. Throughout we shall ignore questions of instrument calibration and atmospheric corrections. Another formula that is suitable is the soil adjusted vegetation index (SAVI) (Huete, 1988), given by

$$\text{SAVI} = 1.5 \cdot \frac{R_2 - R_1}{R_2 + R_1 + 0.5} \quad (2)$$

To the degree that vegetation reflectance may be approximated as a step function (Fig. 1), the two reflectances need not be evenly spaced from the discontinuity, so that measurements by various satellite instruments with different center wavelengths are comparable. Taking

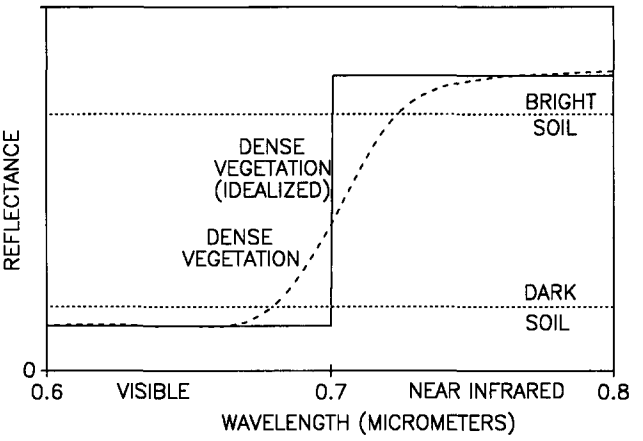

Figure 1. Schematic idealized reflectances are shown for dense live vegetation and bright and dark soil reflectances, and an actual vegetation spectrum.

the change in the logarithm of reflectance as opposed to reflectance itself eliminates the requirement for absolute measurements since only a ratio of reflectances is needed. The ratio of reflectances also partially eliminates geometric considerations of satellite view angle and solar incidence (Holben et al., 1986). However, use of digital counts, as in the NOAA product (Tarpley et al., 1984), yields a slight discrepancy compared with a radiance-based formula (Price, 1987). If the soil reflectance is constant with wavelength in the domain of interest, then the magnitude of the soil reflectance generally has only a minor effect on NDVI.

The significance of NDVI is clear when the background reflectance of soil is independent of wavelength, in which case the numerical value of NDVI increases steadily from near 0 as bare soil is covered by a growing vegetation canopy. The NDVI has the great advantage that no auxiliary information is required besides the measurements of reflectance or radiance. It has several disadvantages: 1) The NDVI is an ad hoc prescription with no explicit physical relationship to vegetation measures such as biomass or LAI, or to radiative transfer calculations, and 2) it is subject to variability associated with soil background brightness (Huete, 1988; Huete and Tucker, 1991). If soil reflectance were constant with wavelength in this spectral region, then its effect on NDVI would nearly cancel in the numerator of Eq. (1), while its effect on the denominator is small for relatively dark soils. However, soil brightness variations do occur, and soil reflectance generally increases with increasing wavelength in this spectral region. Discrepancies from a constant reflectance value limit the validity of Eq. (1) for describing vegetation growing on different reflectivity soils, especially when vegetation cover is low.

Figure 2 presents histograms of soil NDVI and SAVI values corresponding to measurements in Landsat Thematic Mapper (TM) Bands 3 and 4 at 0.63–0.69 μm

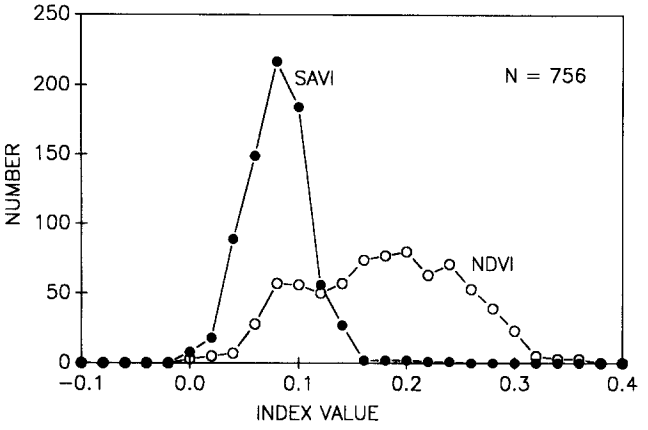

Figure 2. The number of soil reflectance spectra having given values of NDVI and SAVI are illustrated at intervals of 0.01 μm.

and 0.76–0.90 μm, respectively, where the data sets used are discussed later in this paper. Figure 2 illustrates soil variability of about 0.1 for NDVI or 0.05 for SAVI, suggesting that NDVI and other vegetation indices to estimate vegetation conditions should be adjusted for variable soil reflected radiation when deriving remote estimates of vegetation condition. Both indices have a formal range [−1., +1.]. Baret and Guyot (1991) used the SAIL model (Verhoef, 1984) to discuss the sensitivity of seven vegetation index formulas to various approximations and to changes in soil reflectance and leaf inclination. Since that time, the subject of radiometric vegetation indices has continued to flourish, with the goal of finding a formula that is independent of all variables except the presence and amount of vegetation. However, it is not physically possible to eliminate soil reflectance variations, either explicitly or implicitly, from such formulas because soil reflectance *does* affect observed radiances. Also, scaling a radiometric vegetation index to a plant canopy parameter requires, at a minimum, knowledge of the reflectance of a vegetation canopy thick enough to be independent of the underlying soil. Given knowledge of such limiting visible and near infrared reflectance values $r_{\infty 1}$ and $r_{\infty 2}$, the formula [P1, Eq. (12)]

$$\mathrm{VI} = \frac{R_2 - aR_1 - b}{r_{\infty 2} - ar_{\infty 1} - b} \tag{3}$$

satisfies the conditions for a radiometric index, where a and b are the slope and intercept of the visible to the near-IR soil reflectance line,

$$R_2 = aR_1 + b \tag{4}$$

In P1 and P2 the soil line constants a and b were either assumed known, or derived from remotely sensed data. However, in general, a and b are *not* known, and some means for estimating them must be given, as described later. In R_1, R_2 space lines of constant VI are parallel to the soil line. The VI result may then be associated with vegetation properties such as biomass, chlorophyll amount, etc. by an empirical relationship, leaving the resultant radiometric index an empirical description of vegetation with range 0–1. In fact, Eq. (3) has a simple interpretation in terms of an area which is partially covered with dense vegetation (fraction $f = \mathrm{VI}$), with the rest bare soil (fraction $1 - f$).

A Biological Vegetation Index

Leaf area index (LAI) is a fundamental physical attribute of plant canopies which does not require radiometric measurements, but should be an important factor in determining them, given that the appearance of most vegetation is dominated by the leaves, and that the leaves contain the major fraction of chlorophyll, which provides energy input to plants. The two-stream formulation for radiative transfer yields a relation between LAI and observed reflectances. Papers P1 and P2 present the two-stream solution for a vegetation canopy above soil, in a form suitable for experimental verification (see also Smith, 1983; Richardson and Wiegand, 1977). Paper P1 shows that LAI may be inferred from reflectance measurements just above the vegetation canopy, given knowledge of r_s, r_∞, and c. The reflectances R must be measured sufficiently far above a vegetation canopy so that variability associated with the individual leaves and plant structure is negligible. The resultant reflectance above the canopy is given by

$$R = (r_\infty + D/r_\infty)/(1 + D), \tag{5}$$

where

$$D = \frac{r_s - r_\infty}{1/r_\infty - r_s} \cdot e^{-2c \cdot \mathrm{LAI}}. \tag{6}$$

The quantities r_s, r_∞, and c are all functions of wavelength. The quantity r_∞ may be obtained from radiation measurements of a dense canopy (extrapolated from lower LAI values), while c may be obtained either from measurements of the attenuation of radiation within a canopy, or by considering a canopy at varying stages of growth, assuming that the evolution of canopy structure during growth does not change the interaction with radiation.

Figure 3 illustrates the sensitivity of this formulation to soil brightness values. For dark soils the visible measurement is relatively insensitive to changes in the vegetation cover, while the infrared measurement is quite sensitive to changes in this quantity. Conversely, for bright soils the decrease in visible reflectance as vegetation increases is rather large, yielding a sensitive measurement of LAI, while the sensitivity of the infrared measurement to LAI is poor. If r_∞, r_s, and c are all known (at a particular wavelength), then a single reflectance measurement permits inference of LAI, except for saturation at large LAI. Saturation occurs at all wavelengths

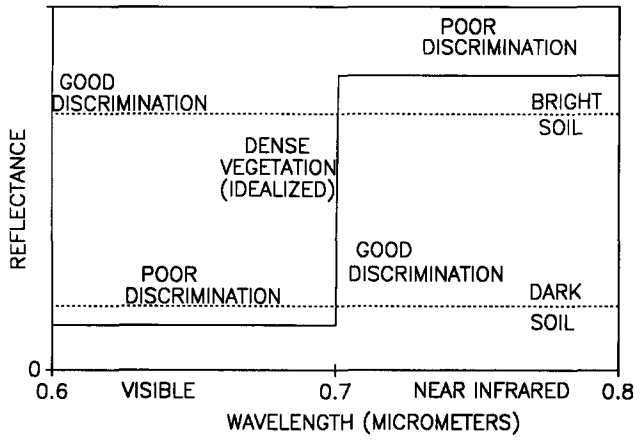

Figure 3. Zones of good and poor discrimination of leaf area index are illustrated in the visible and near-infrared for crops grown on bright and dark soil backgrounds.

for large LAI, effectively limiting the sensitivity of *all* radiometric vegetation indices for dense vegetation cover.

For reference it is useful to develop an approximate form of Eqs. (5) and (6), namely (Baret and Guyot, 1991; Clevers, 1988),

$$R \simeq R' = r_\infty + (r_s - r_\infty)\cdot e^{-2c\cdot LAI}$$
$$= r_\infty + D/r_\infty - r_s D. \qquad (7)$$

The relative error in approximating the reflectance by Eq. (7) may be found by taking the difference between Eq. (7) and Eqs. (5) and (6),

$$\Delta R = R' - R = (r_\infty + D/r_\infty)\cdot[1 - 1/(1+D)] - r_s D$$
$$= (r_\infty D + D^2/r_\infty)/(1+D) - r_s D,$$

so that

$$\frac{\Delta R}{R} = D - \frac{r_s(D+D^2)}{r_\infty + D/r_\infty}. \qquad (8)$$

The maximum relative error of $(\Delta R/R)$ may be found by setting the derivative with respect to LAI equal to zero, where from the chain rule $\partial/\partial \mathrm{LAI} = \partial/\partial D\cdot(\partial D/\partial \mathrm{LAI})$. Thus

$$\frac{\partial(\Delta R/R)}{\partial \mathrm{LAI}} = \left[1 - \frac{r_s(1+2D)}{r_\infty + D/r_\infty} + \frac{r_s(D+D^2)/r_\infty}{(r_\infty + D/r_\infty)^2}\right]\cdot\frac{\partial D}{\partial \mathrm{LAI}} = 0,$$

which yields D at which the maximum difference between the approximate form [Eq. (7)] and the exact [Eqs. (5) and (6)] is given by

$$D(\text{max error}) \simeq r_\infty^2\left(-1\left[\frac{r_s r_\infty}{1 - r_s r_\infty}\cdot\left(\frac{1}{r_\infty^2 - 1}\right)\right]^2\right).$$

Substituting into Eq. (8) yields an expression for this error. Assuming value $r_s \simeq 0.2$ and values for r_∞ as given in Table 1, as discussed later, the resulting error is of order 0.3% in the visible and order 4% in the infrared. For the most reflective soil, as discussed later, the error is 12% in the infrared. Accordingly, Eq. (7) may be used in the visible wavelengths and, for error estimation, in the near-infrared. For inference of LAI the exact expression is used in the infrared because even the 12% correction may be an underestimate as compared to other soil reflectances or vegetation types or observation conditions.

Table 1. Values of Limiting Reflectance ($r_{\infty i}$, Decimal) and Attenuation Coefficient (c) for Corn

	Spectral Band			
Variable	*TM 1*	*TM 2*	*TM 3*	*TM 4*
r_∞	0.030	0.055	0.036	0.52
c	.694	.661	.700	.255

At this point the accuracy and indeed the applicability of the two-stream theory have not been verified by field measurements. Two potential problems are apparent: a) The two-stream formulation of P1 and P2 assumes the same constants for both upward and downward propagating radiation, despite the fact that some plant canopies do not have this symmetry, and b) to be useful, the same constants must apply throughout the growth of the plants, despite evident changes in canopy architecture from seeding to mature stages for many types of vegetation. If r_∞ and/or c change during plant development, then the theory becomes an empirical fit of reflectance measurements using two parameters which depend on the growth stage, and hence on LAI. Therefore, the applicability of theory must be verified either against more general descriptions of radiation interaction with a plant canopy, such as the SAIL model (Verhoef, 1984), or else, as here, with field data.

Experimental Measurements of Corn

Reflectance measurements for the four Thematic Mapper bands, 0.45–0.52 μm, 0.52–0.60 μm, 0.63–0.69 μm, and 0.76–0.90 μm, were carried out for corn (*Zea mays* L.) during the 1991 growing season (Bausch, 1993). Four different soils were placed under the vegetation canopy while repeated reflectance measurements were obtained as the crop developed. A full description of the experimental procedure is given in that paper. For the present purposes the limitations of the data are a) only one vegetation type and b) radiation measurements in a single configuration—measurement toward nadir, solar zenith angle of approximately 19° (Bausch, 1993, Table 1). In other respects, the experimental design is ideal for testing the two-stream theory. If theory applies, then the value of c in each of the four Thematic Mapper bands should remain constant throughout the growing season, independent of brightness differences among the underlying soils. However, one among the four soil backgrounds has visible reflectances essentially equal

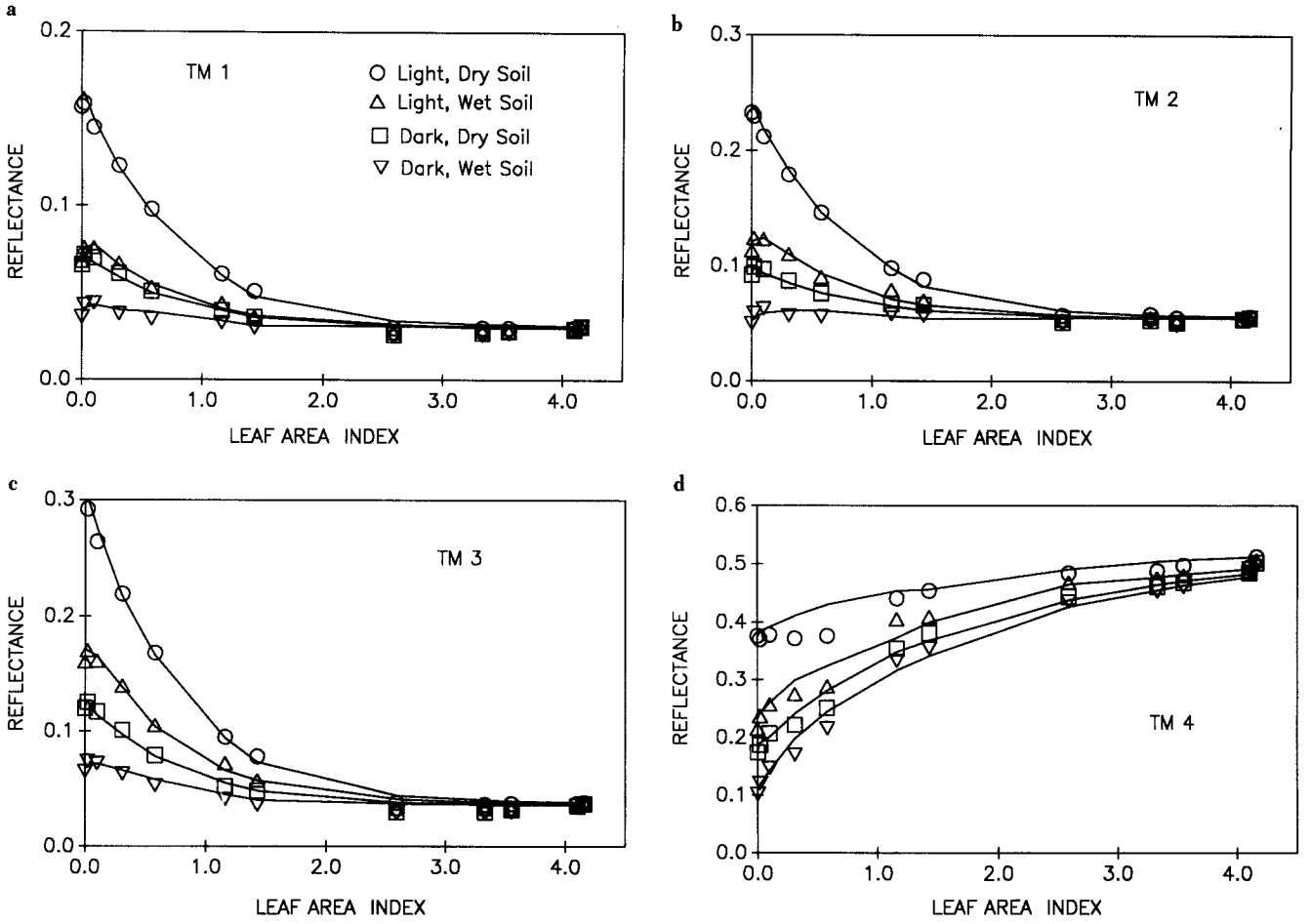

Figure 4, a–d. Seasonal measured reflectances in four TM bands are presented for the composite corn canopy–soil background with four different soils beneath the canopy. Backgrounds are identified in 4a.

to those of vegetation, so that no discrimination is possible in this spectral channel. This case (dark soil, wet) was eliminated from the analysis of TM Bands 1–3. The limiting value for vegetation reflectance in each waveband was obtained by examination of a plot of the reflectance data, although these data do not quite reach the saturation point in the near infrared, TM Band 4, where the highest LAI value is 4.16. The estimated limiting values r_∞ are listed in Table 1.

The attenuation coefficient c was determined by a best fit to the time sequence of data for different soil types, i.e., the error expression

$$E = \sum_{\substack{\text{soil}\\ \text{type}}} \sum_{\substack{12\\ \text{obser-}\\ \text{vations}}} [R_{\text{measured}} - R_{\text{theory}}]^2 \qquad (9)$$

was minimized by varying c, where R_{measured} is the measured reflectance and R_{theory} is given by Eqs. (5) and (6), using measured values of LAI and r_s. Minimization by differentiating Eq. (9) with respect to c and solving numerically is straightforward and thus not presented here. Table 1 presents solution values for four Thematic Mapper bands, and the resulting reflectance functions are compared with the observed values in Figure 4a–d. The theoretical reflectance values, indicated by solid lines, are somewhat irregular, due to changes in measured soil reflectance values with time, despite the fact that the soils were not treated or modified during the course of the experiment. This soil variation is assumed to be due to experimental variability and measurement error.

Theory and experiment agree well for all cases. The attentuation coefficients in the visible (TM1–TM3) are larger than in the infrared (TM4) because the absorption is higher in the visible than in the infrared while transmission and reflection are smaller. However, the objective is not to determine proper values for r_∞ and c, but to establish the ability to infer LAI from the radiometric measurements, given numerical values of these constants. To this end, Eqs. (5) and (6) may be solved for LAI yielding

$$\text{LAI} = \frac{1}{2c} \ln \left[\frac{R - 1/r_\infty)(r_s - r_\infty)}{(R - r_\infty)(r_s - 1/r_\infty)} \right]. \qquad (10)$$

Comparison of LAI calculated from measured R with values obtained by measurement of leaves of individual

plants shows good agreement, as indicated by goodness of fit for Figures 4a–d, with several limitations:

a. In the original experiment it was necessary to make repetitive radiometric measurements of a single site in order to identify effects of differing soil backgrounds, while eliminating possible variations in stand density from one location to another. This required measurement first of the reflectances of trays of soil in an open area, then measurement of corn reflectance after these trays were placed under the vegetation canopy. Use of Eq. (10) for LAI prior to vegetation growth shows a discrepancy of 0.05–0.1 in radiance-derived LAI. Evidently this discrepancy is associated with the experimental procedure, including both radiometry and any effects from moving the trays of soil.
b. At limiting LAI values, corresponding to LAI > 2 in TM Channels 1–3 and LAI > 3 in TM Channel 4, Eq. (10) is insensitive to LAI changes, so that experimental errors produce large changes in predicted LAI.
c. The performance of Eq. (10) depends on the difference in reflectance between the soil and dense vegetation, as illustrated in Figure 3. Thus the dark soil, wet, is unsuitable for estimation of LAI in TM Channels 1–3, while the bright soil, dry, is relatively poor for estimation of LAI in TM Channel 4.
d. Finally, soil brightness is highly variable in space, and its value is not generally known. Therefore, solution relying on Eq. (10) at a single wavelength is unsatisfactory for broad area applications such as remote sensing, and consideration of two or more spectral channels including visible and near-infrared is required.

Given these limitations, the validity of Eqs. (5) and (6) is summarized as follows: Given qualifications a–d above, the radiometric estimation of LAI yields an error comparable to uncertainties associated with field measurement of LAI. This is due to the fact that samples of adjacent crop areas were used to measure LAI, in order to avoid destruction of the area used for radiometric measurements during the growing season. Thus theory and measurement are judged to agree, to within experimental precision. However, consideration of two or more spectral channels is necessary for radiometric estimation of LAI because the background soil reflectance is generally not known.

DESCRIBING WAVELENGTH DEPENDENCE OF SOIL REFLECTANCE

Although Eq. (10) provides LAI from a single measurement R, given r_s, this solution is not generally usable because r_s is spatially variable, and somewhat dependent on time through moisture dependence. In P1, approximations to Eqs. (5) and (6) for both visible and near-infrared wavelengths, plus Eq. (4), were used to obtain LAI in terms of measured reflectances. Thus Eqs. (5) and (6) were solved for r_s in terms of reflectances measured above the canopy, where subscripts i, j, k will be used to indicate wavelength dependence:

$$r_{si} = [r_{\infty i} + U_i / r_{\infty i}] / (1 + U_i), \tag{11}$$

where

$$U_i = \frac{R_i - r_{\infty i}}{1 / r_{\infty i} - R_i} \cdot e^{2c_i LAI}. \tag{12}$$

Equation (5) and the definition of D (for downward looking) and Eq. (11) and U (for upward looking) are inverses, with D, a function of r_s, the soil reflectance beneath the canopy and U, a function of R, the reflectance measured above the canopy. Equations (11) and (12), for two wavelengths, plus Eq. (4), may be solved numerically or, in special cases, analytically (P1). In P2 constants equivalent to a,b were obtained from a scattergram of satellite image data for an area containing pure pixels of bare soil. However, pure soil pixels often may not be present, especially for instruments with lower spatial resolution such as the NOAA Advanced Very High Resolution Radiometer at 1.1 km. Therefore, a more general relation among reflectances at different wavelengths is required. These empirical relations are developed among reflectances in the visible and near-infrared, using an ensemble of measured soil reflectances.

Generally, soil reflectance increases with wavelength in the range 0.5–1.1 μm. In considering high resolution spectra of U.S. soils (Stoner et al., 1980), Price (1990, Figs. 2 and 3) found that 74% of the spectral variability was described by a spectral shape that increased linearly in this spectral range, while the next 22% of spectral variability was low in amplitude and relatively linear with wavelength in the 0.5–1.1 μm spectral region. Thus, reflectance at a single wavelength may be used to predict reflectance in another wavelength band, with relatively small residual error; the error is reduced further if two wavelength bands are used to predict reflectance in a third band.

The relations sought were obtained by statistical analysis of three collections of soil reflectance spectra. The first consisted of 545 spectral measurements of wet (0.1 bar moisture tension) soils (Stoner et al., 1980), where the domain of measurement was 0.55–2.31 μm. The second consisted of 128 samples measured in the domain 0.4–2.5 μm (Satterwhite and Henley, 1991), representing both wet and dry soil samples. The third consisted of 81 soil samples measured in the domain 0.4–2.5 μm, with all spectra measured for dry soils (Sets, 1990). The three groups of high resolution reflectance spectra were convolved with the instrument functions (spectral weighting functions) for the Thematic Mapper

Table 2. Equations Describing Soil Reflectance (Decimal) in a Satellite Band in Terms of Reflectances in Other Satellite Spectral Bands

Equation	*Standard Error of Estimate*
One Predictor	
TM3 = −0.029 + 0.89·TM4	0.017
MSS5 = −0.035 + 0.86·MSS7	0.021
HRV2 = −0.030 + 0.88·HRV3	0.017
AVHRR1 = −0.028 + 0.85·AVHRR2	0.018
Two Predictors	
TM3 = −0.011 + 0.43·TM4 + 0.63·TM2	0.008
MSS5 = −0.017 + 0.44·MSS7 + 0.66·MSS4	0.012
HRV2 = −0.018 + 0.52·HRV3 + 0.56·HRV1	0.010

in order to derive reflectances equivalent to those seen by that instrument, as well as other instruments which are mentioned later. Multiple linear regression yielded relationships among the reflectance values (range 0.0–1.0) in the form

$$r_{si} = z_0 + z_1 r_{sj} + z_2 r_{sk} \tag{13}$$

for both single variable predictors ($z_2 = 0$) and two variable predictors (both z_1 and z_2 nonzero). Three equations are possible by permuting the three spectral channels. Table 2 presents the preferred relationships for the Landsat Thematic Mapper and MultiSpectral Scanner (MSS), SPOT high resolution video (HRV), and NOAA Advanced Very High Resolution Radiometer (AVHRR), where the root mean square error is given in the right-hand column. In order to reduce confusion, the reflectance relationships are given in terms of the common "names" of the spectral channels, rather than as repeated versions of Eq. (13).

The errors listed do not correspond to the error resulting when Eqs. (11) and (12) are inserted into Eq. (13) to estimate LAI from radiance measurements. However, this error in LAI due to soil reflectance error may be estimated by substituting the approximate form of the radiance solution [Eq. (7)] into Eq. (13):

$$\begin{aligned} r_{\infty i} + (R_i - r_{\infty i})e^{2c_i LAI} \\ = z_0 + z_1[r_{\infty j} + (R_j - r_{\infty j})e^{2c_j LAI} \\ + z_2[r_{\infty k} + (R_k - r_{\infty k})e^{2c_k LAI}]. \end{aligned} \tag{14}$$

The theoretical value of leaf area index (LAI′), given an error in soil reflectance δr_{si}, results from solution of the equation

$$\begin{aligned} \delta r_{si} + r_{\infty i} + (R_i - r_{\infty i})e^{2c_i LAI'} \\ = z_0 + z_1[(r_{\infty j} + (R_j - r_{\infty j})e^{2c_j LAI'}] \\ + z_2[r_{\infty k} + (R_k - r_{\infty k})e^{2c_k LAI'}]. \end{aligned} \tag{15}$$

Subtracting Eq. (14) from (15), expanding exponentials with $\delta\text{LAI} = \text{LAI}' - \text{LAI}$, and then using Eq. (7) to eliminate the exponential terms yields

$$\frac{\delta \text{LAI}}{\delta r_{si}} = \frac{1}{2[z_1 c_j (r_{sj} - r_{\infty j}) + z_2 c_k (r_{sk} - r_{\infty k}) - c_{si}(r_{si} - r_{\infty i})]}. \tag{16}$$

Then $(\delta\text{LAI} / \delta r_{si}) \cdot \delta r_{si}$ gives the resulting error in LAI, as listed on the right in Table 2. For estimation purposes a value of 0.20 is used for soil reflectance. When the three possible sets of equations for TM2, TM3, and TM4 are considered and resulting errors compared, it is found that the selections in Table 2 are best, although only marginally better than equations representing the prediction of the near-infrared Channel TM4 by the visible channels, TM2 and TM3. The interpretation of Table 2 is straightforward: The one-parameter equations represent "best fit" soil lines for the ensemble of soil spectra, while the two-variable parameter equations represent an estimate of reflectance of TM3 from TM2 and TM4. By comparison of the two error values the two-channel predictors reduce residual error by approximately 50% compared with the single predictor.

A question remains as to the generality of the equations in Table 2, i.e., the representativeness of the errors. This was studied by dividing the ensemble into two groups, the first consisting of the LARS spectra, obtained for wet soils, the second for the remaining (Corps of Engineers, SETS) spectra. Regression equations were derived for each group separately, then applied to the other data set. The LARS spectra had generally low reflectances (e.g., mean of 0.13 in TM4) while the others had high reflectances (mean of 0.31 in TM4). Thus the LARS equations are extrapolated to high reflectance values when applied to the dry soils, leading to a r.m.s error of order 0.04 in predicting Channel TM3 from one predictive variable, 0.02 from two variables. The high reflectance soil equations for both one and two predictive variables lead to an error of order 0.015 when applied to the LARS soils. For comparison, the mean soil reflectance in TM3 for the ensemble of 756 spectra is 0.18, with a standard deviation of 0.11. As an additional check the full ensemble TM equations were applied to the Bausch (1993) soil reflectance measurements. The resulting error in TM3 for the four soils was (.003, .007, .007, .002) for the single-channel predictor and (.002, .003, .006, .003) for the two channel predictor.

The soil prediction equations for other satellite instruments are also given in Table 2. Although the Bausch data represent only the four TM spectral channels, Figures 1 and 3 suggests that results may be applied to other spectral bands. Because the LARS soils do not span the spectral domain of the MSS4 and HRV1 channels, the weighting functions for these instruments were

truncated at 0.55 μm to permit the calculations. The errors resulting from use of the full ensemble and partitions are similar to those for the Thematic Mapper. The MSS equations were developed for MSS5 for one predictive variable (MSS7) and for two variables (MSS4 and MSS7), where the channel numbering is from the early Landsat satellites. The MSS6 channel was excluded from analysis because it partly spans the vegetation rise of reflectance at 0.7 μm, creating uncertainty for parameters $r_{\infty i}$ and c_i for this spectral interval. The generality of the MSS equations was tested as with TM by dividing the ensemble into wet (LARS) spectra and wet and dry spectra, as before, with similar results. As an additional check, the data sets of Huete et al. (1984) containing soil reflectance data for the MSS channels were inserted into the equations in Table 2 in order to provide an independent estimate of error. Among the 20 soils in Huete et al. (1984, Table 5), 15 are different from those in the LARS data set, while five belong to similar soil series. The resulting errors for MSS5 from the equations in Table 2 are 0.011 for a single-channel predictor, 0.013 for the two-channel predictor.

In summary, the error in using equations in Table 2 to predict the visible soil reflectance is estimated at 0.03 for a single channel predictor (visible from near-infrared) and 0.015 for visible by two channel prediction. This leads from Eq. (16) to an error estimate for LAI of 0.1 for both one- and two-channel predictors, which is comparable to errors in field measurement. The larger error in soil reflectance prediction by only one variable is compensated by lower sensitivity of the LAI solution to this error.

RADIATION SOLUTION FOR LEAF AREA INDEX

From the preceding analysis the radiometric estimate of LAI results from solution of the soil equation $r_{s3} = z_0 + z_1 r_{s4} + z_2 r_{s2}$, after substitution of the radiation deserved values [Eqs. (11) and (12)],

$$\begin{aligned} r_{\infty 3} + (R_3 - r_{\infty 3}) e^{2c_3 LAI} \\ = z_0 + z_1[(r_{\infty 4} + U_4 / r_{\infty 4}) / (1 + U_4)] \\ + z_2[r_{\infty 2} + (R_2 - r_{\infty 2}) e^{2c_2 LAI}], \end{aligned} \quad (17)$$

where

$$U_4 = \frac{R_4 - r_{\infty 4}}{1 / r_{\infty 4} - R_4} \cdot e^{2c_4 LAI}.$$

For remote sensing applications involving large amounts of data, it is inefficient to solve Eq. (17) repeatedly for each location (pixel). In P2 a lookup table procedure was described that permits rapid evaluation of LAI from visible and near-infrared reflectance values. However, in the present case, Eq. (17) contains *three* radiance values, R_2, R_3, and R_4, corresponding to three channels of the Thematic Mapper. Because c_2 and c_3 are nearly equal (Table 1) Eq. (17) may be reduced to two variables. First, let $\bar{c} = (c_2 + c_3)/2$ and $\delta c = (c_3 - c_2)/2$, and expand the exponential term in $\exp(\delta c \cdot \mathrm{LAI})$, keeping only the first term. To simplify further, define $\alpha = (r_{\infty 3} - z_2 r_{\infty 2} - z_0)/z_1$, $\beta = [R_3 - r_{\infty 3} - z_2(R_2 - r_{\infty 2})]/z_1$, and $\gamma = 2\beta \cdot \delta c$. In numerical computations the value of β must be limited to positive values: Instrumental errors and anomalous targets such as clouds can yield negative values of β, but these must be excluded from the LAI solution domain. Then the equation to be solved becomes

$$\alpha + (\beta + \gamma \mathrm{LAI}) e^{2\bar{c} LAI} = (r_{\infty 4} + U_4 / r_{\infty 4}) / (1 + U_4). \quad (18)$$

Following P1 and P2, it is convenient to change variables to $x = e^{2c_4 LAI}$, and to define $p = \bar{c} / c_4$ so that $e^{2\bar{c} LAI} = x^p$. Then, given x_0, the solution to the equation

$$\alpha + \beta x_0^p = (r_{\infty 4} + U_4 / r_{\infty 4}) / (1 + U_4), \quad (19)$$

the full (three reflectance variables) solution may be obtained. This solution x_1, correct to first order in δc, is given by

$$x_1 = x_0 - \gamma x_0^p \cdot \mathrm{LAI}(x_0) / [w(\alpha + \beta x_0^p - 1 / r_{\infty 4}) + \beta p x_0^p], \quad (20)$$

where $w = (R_4 - r_{\infty 4}) / (1 / r_{\infty 4} - R_4)$. However, comparing terms, $\bar{c} = 0.68$, while $\delta c = 0.02$, so that this correction to x_0 is negligible in view of other uncertainties. It is important to note that Eq. (19) is a function of only two independent variables, the measurement R_4 and the quantity $[R_3 - r_{\infty 3} - z_2(R_2 - r_{\infty 2})]$, so that a two-dimensional lookup table describes the domain of input radiation measurements for the lookup table for LAI.

Equation (19) must be solved numerically. From Table 1 the ratio p has the value $0.680 / 0.255 = 2.67$. Using the approximate form [Eq. (7)] for the TM4 channel on the right side of Eq. (19), the result is a polynomial equation which may be solved analytically for $p = 2$ and $p = 3$. Thus Eq. (19) becomes

$$\beta x^p + (r_{\infty 4} - R_4) x + \alpha - r_{\infty 4} = 0. \quad (21)$$

Letting $a_0 = (\alpha - r_{\infty 4}) / \beta$ and $a_1 = (r_{\infty 4} - R_4) / \beta$, the solution for $p = 2$ is

$$x(p = 2) = [-a_1 + (a_1^2 - 4a_0)^{1/2}] / 2$$

and for $p = 3$ (Abramowitz and Stegun, 1964)

$$\begin{aligned} x(p = 3) \\ = [-a_0 / 2 + (a_1^3 / 27 + a_0^2)^{1/2}]^{1/3} \\ + [-a_0 / 2 - (a_1^3 / 27 + a_0^2)^{1/2}]^{1/3}, \end{aligned}$$

and an approximation x_a to the solution of Eq. (21) for an intermediate value of p is given by

$$x_a = (p - 2) \cdot x(p = 3) + (3 - p) \cdot x(p = 2).$$

The trial solutions $x(p = 2)$ and $x(p = 3)$ bracket the correct solution, and x_a is a good starting point for numerical solution of Eq. (19). The procedure described in P2 may then be applied to image data.

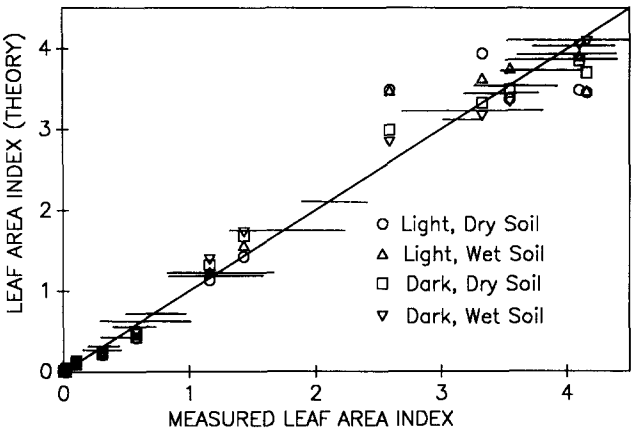

Figure 5. Comparison of LAI estimated from theory with measured LAI for the four Thematic Mapper bands in the study. The errors in field measurement of LAI are shown on the 1:1 line.

An example provides the logical sequence to the solution for LAI. From measured reflectances (TM2,3,4 = 0.0699, 0.0568, 0.409), the infinite reflectance values from Table 1 ($r_{\infty 2,3,4} = 0.036$, 0.055, 0.52), and the soil coefficients from Table 2 with two predictors ($z_0 = -0.11$, $z_1 = 0.43$, $z_2 = 0.63$) one may compute $a = 0.0287$, $\beta = 0.0265$, after which $a_0 = -18.51$ and $a_1 = 4.17$. Substitution into the expressions following Eq. (21) yields $x(p=2) = 2.696$, $x(p=3) = 2.125$, and $x_a = 2.507$. These three values are used for input to the numerical solution of Eq. (21), with the result x(numerical) = 2.211, LAI = 1.56. The measured reflectances were obtained above the light, dry soil background, with LAI estimated as 1.43 from ground data.

Figure 5 illustrates the relation of field measured LAI and values derived from the reflectance measurements, where results from the theoretical formulation are indicated by symbols. Estimated experimental errors in the field measurements are used to bracket the 1:1 line. As described earlier, the accuracy of the radiometric estimate deteriorates as the leaf area index exceeds 3. The fact that experimental errors contribute to the discrepancy between radiometric and biological estimates of LAI is shown in Figure 6, illustrating measurements of the most reflective bare soil ("light, dry") for the three pertinent thematic mapper bands, as well as the measured reflectance values above the plant canopy as the crop developed. The soil reflectance variability belies the assumption that the soil underlying vegetation at a specific point has an unvarying reflectance.

Figure 6. Seasonal variation of the bare soil and corn reflectances are illustrated, showing that soil reflectances varied in time during the experiment.

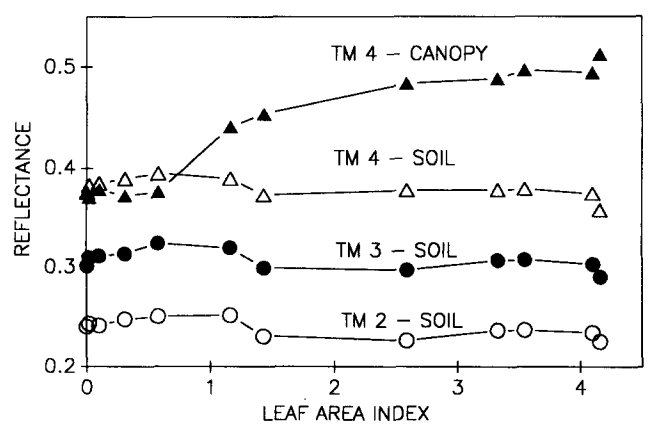

Because the range of LAI is inconvenient, namely $(0, \infty)$, it is desirable to define (P2) a leaf vegetation index V_L, a function of LAI, by

$$V_L = 1 - e^{-2c_4 \mathrm{LAI}}, \tag{22}$$

which has values V_L (LAI = 0) = 0 and V_L (LAI = ∞) = 1. The infrared channel scaling (c_4) is preferred as it causes V_L to approach saturation more slowly than the visible channels. The inverse of Eq. (22) is

$$\mathrm{LAI} = -\frac{1}{2c_4}\ln(1 - V_L). \tag{23}$$

For small values of LAI an error of 0.1 in LAI corresponds to an error in V_L of $\delta V_L \approx c_4 \delta \mathrm{LAI} = 0.03$.

If we identify the product $c_4 \cdot$ LAI with optical depth in the infrared, then this product may be more indicative of important vegetation quantities than LAI itself because it represents the chlorophyll amount per leaf area, which probably varies for leaves of different plant species. Thus LAI may not have the same significance for grasses, broadleaf species, succulents, etc., while V_L may be a better indicator of important vegetation characteristics.

SENSITIVITY TO ERRORS IN REFLECTANCE MEASUREMENT

The radiometric estimate of LAI is affected by errors in the measurement of reflectance. The magnitude of these errors may be obtained from Eq. (21). By differentiation of the measured reflectance values R_2, R_3, and R_4 with respect to LAI, these relationships are

$$\frac{1}{z_1}\frac{\partial R_3}{\partial \mathrm{LAI}}x^p + \beta\frac{dx^p}{d\mathrm{LAI}} + (R_4 - r_{\infty 4})\frac{dx}{d\mathrm{LAI}} = 0,$$

$$\beta\frac{dx^p}{d\mathrm{LAI}} - x\frac{\partial R_4}{\partial \mathrm{LAI}} + (r_{\infty 4} - R_4)\frac{dx}{d\mathrm{LAI}} = 0,$$

$$\frac{\partial R_3}{\partial \mathrm{LAI}} = -z_2\frac{\partial R_2}{\partial \mathrm{LAI}}.$$

Using the definitions $dx^p/d\mathrm{LAI} = 2\bar{c}x^p$ and $dx/d\mathrm{LAI} = 2c_4x$, and after some manipulation,

$$\frac{\partial \mathrm{LAI}}{\partial R_2} = -z_2 \frac{\partial \mathrm{LAI}}{\partial r_3} = \frac{-z_2 x^{p-1}}{2z_1[c_4(R_4 - r_{\infty 4}) - \bar{c}\beta x^{p-1}]},$$

$$\frac{\partial \mathrm{LAI}}{\partial R_4} = \frac{1}{2[\bar{c}\beta x^{p-1} - c_4(R_4 - r_{\infty 4})]}.$$

These expressions may be evaluated at several limiting values. At $x = 1$, corresponding to LAI = 0,

$$\left.\frac{\partial \mathrm{LAI}}{\partial R_2}\right|_{LAI=0} = -z_2 \left.\frac{\partial \mathrm{LAI}}{\partial R_3}\right|_{LAI=0} = -\frac{z_2}{z_1}\left.\frac{\partial \mathrm{LAI}}{\partial R_4}\right|_{LAI=0}$$

$$= \frac{-z_2}{2[z_1 c_4(R_4 - r_{\infty 4}) - \bar{c}(R_3 - r_{\infty 3}) + \bar{c}z_2(R_2 - r_{\infty 2})]}.$$

Using the relationship between the soil reflectances [Eq. (13), where $i = 2, j = 4, k = 3$] this expression reduces to

$$\frac{\partial \mathrm{LAI}}{\partial R_2} = \frac{z_2}{2[(r_{\infty 3} - z_2 r_{\infty 2} - z_0) - z_1 c_4 r_{\infty 4} + z_1(c_4 - \bar{c})R_4]}$$

$$\approx \frac{z_2}{2z_1(\bar{c} - c_4)R_4}$$

$$= \frac{0.63}{2 \cdot 0.43 \cdot (0.70 - 0.26)R_4} = \frac{1.7}{R_4}.$$

Thus for a soil reflectance in TM4 of 0.2 $\partial \mathrm{LAI} / \partial R_2 \approx 9$, and an error of 0.01 in R_2 results in an error of order 0.1 in the estimate of LAI.

For $x \to \infty$ corresponding to LAI $\to \infty$, the expressions reduce to

$$\left.\frac{\partial \mathrm{LAI}}{\partial R_2}\right|_{LAI=\infty} = -z_2 \left.\frac{\partial \mathrm{LAI}}{\partial R_3}\right|_{LAI=\infty}$$

$$\to \frac{-z_2}{2\bar{c}[(R_3 - r_{\infty 3}) - z_2(R_2 - r_{\infty 2})]},$$

$$\left.\frac{\partial \mathrm{LAI}}{\partial R_4}\right|_{LAI=\infty} \to \frac{1}{2\bar{c}(R_4 - r_{\infty 4})}$$

so that the solution for LAI becomes increasingly sensitive to measurement errors as $R_2 \to r_{\infty 2}$, $R_3 \to r_{\infty 3}$, and $R_4 \to r_{\infty 4}$.

CONCLUSION AND LIMITATIONS

The analysis shows that the simple two-stream radiation theory provides an adequate description of reflectance of corn above a variable soil background. Relationships among soil reflectance values have been developed. This permits inversion of the reflectance / LAI radiation problem, with a solution which is well behaved except as LAI $\to \infty$. However, a number of significant limitations apply to the inversion procedure.

1. The atmosphere has been neglected, making the treatment unsuited for application to satellite data. Further analysis is needed.
2. The constants derived, r_∞ and c, apply only to corn for the viewing conditions of the experiment. Further experimental work is necessary.
3. As in P1 and P2, the assumption of the soil background is not generally valid, especially in natural areas, as opposed to cropland, and for those farmed areas where no-till practices are used, which leave the soil covered with crop residue. In such regions, where dead vegetation and litter cover the ground, the soil relationships need to be replaced with a "litter" or "understory" equation, assuming that such a surface layer is reasonably uniform within the area of interest. Perhaps multispectral observations can be used to discriminate the vegetation types, and to help in the selection of proper values for such backgrounds.

We are indebted to Craig Wiegand and John Norman and a reviewer for helpful criticism of the manuscript.

REFERENCES

Abramovitz, M., and Stegun, I. A. (1964), *Handbook of Mathematical Functions*, U.S. Department of Commerce, Washington, DC, pp. 17, 18.

Baret, F., and Guyot, G. (1991), Potentials and limits of vegetation indices for LAI and APAR assessment, *Remote Sens. Environ.* 35:161–174.

Bausch, W. C. (1993), Soil background effects on reflectance-based crop coefficients for corn, *Remote Sens. Environ.* 46: 213–222.

Clevers, J. G. P. W. (1988), The derivation of a simplified reflectance model for the estimation of leaf area index, *Remote Sens. Environ.* 25:52–69.

Clevers, J. G. P. W. (1989), The application of a weighted infrared-red vegetation model for estimating leaf area index by correcting for soil moisture, *Remote Sens. Environ.* 29: 25–37.

Hall, F. G., Huemmrich, K. S., Goetz, S. J., Sellers, P. J., and Nickeson, J. E. (1992), Satellite remote sensing of surface energy balance: success, failures, and unresolved issues in FIFE, *J. Geophys. Res.* 97:19,061–19,089.

Holben, B. N., Kimes, D. S., and Fraser, R. S. (1986), Directional reflectance in AVHRR red and near-IR bands for three cover types and varying atmospheric conditions, *Remote Sens. Environ.* 19:213–236.

Huete, A. R. (1988), A soil adjusted vegetation index (SAVI), *Remote Sens. Environ.* 25:295–309.

Huete, A. R., and Tucker, C. J. (1991), Investigation of soil influences in AVHRR red and near-infrared vegetation index imagery, *Int. J. Remote Sens.* 12:1223–1242.

Huete, A. R., Post, D. F., and Jackson, R. D. (1984), Soil spectral effects on 4-space vegetation discrimination, *Remote Sens. Environ.* 15:155–165.

Perry, C. R., and Lautenschlager, L. F. (1984), Functional equivalence of spectral vegetation indices, *Remote Sens. Environ.* 14:169–182.

Price, J. C. (1987), Calibration of satellite radiometers and the comparison of vegetation indices, *Remote Sens. Environ.* 21:15–27.

Price, J. C. (1990), On the information content of soil reflectance data, *Remote Sens. Environ.* 33:113–121.

Price, J. C. (1992), Estimating vegetation amount from visible and near infrared reflectance measurements, *Remote Sens. Environ.* 41:29–34.

Price, J. C. (1993), Estimating leaf area index from satellite data, *IEEE Trans. Geosci. Remote Sens.* 31:727–734.

Richardson, A. J., and Wiegand, C. L. (1977), Distinguishing vegetation from soil background information, *Photogramm. Eng. Remote Sens.* 43:1541–1552.

Rouse, J. W., Haas, R. H., Schell, J. A., Deering, D. W., and Harlan, J. C. (1974), Monitoring the vernal advancement of natural vegetation, NASA / GSFC Final Report, Greenbelt, MD, 371 pp.

Satterwhite, M. B., and Henley, J. P. (1991), Hyperspectral signatures (400–2500 nm) of vegetation, minerals, soils, rocks, and cultural features: laboratory and field measurements, U.S. Army Corps of Engineers, ETL-0573, Fort Belvoir, VA.

Sets, Inc. (1990), *Spectral Catalog,* Milalane, HA, 5 Vols.

Smith, J. A. (1983), Matter-energy interaction in the optical region, in *Manual of Remote Sensing,* 2nd ed., American Society of Photogrammetry, Falls Church, VA, Vol. 1, pp. 61–113.

Stoner, E. R., Baumgardner, M. F., Biehl, L. L., and Robinson, B. F. (1980), *Atlas of Soil Reflectance Properties,* Research Bulletin 862, Purdue University, West Lafayette, IN.

Tarpley, J. D., Schneider, S. R., and Money, R. L. (1984), Global vegetation indices from the NOAA-7 meteorological satellite, *J. Clim. Appl. Meteorol.* 23:491–494.

Verhoef, W. (1984), Light scattering by leaf layers with application to canopy reflectance modeling: the SAIL model, *Remote Sens. Environ.* 16:125–141.

Wiegand, C. L., and Richardson, A. J. (1990), Use of spectral vegetation indices to infer leaf area, evapotranspiration and yield: rationale and results, *Agron. J.* 82:623–629.